Kinetics and Catalysis, Vol. 43, No. 4, 2002, pp. 573–579. Translated from Kinetika i Kataliz, Vol. 43, No. 4, 2002, pp. 621–627.

Effect of the Conditions of Thermal Treatment of Molybdenum–Titanium and Vanadium–Molybdenum–Titanium Oxide Catalysts on Pore Structure Formation

G. A. Zenkovets, V. Yu. Gavrilov, G. N. Kryukova, S. V. Tsybulya, and V. N. Parmon

Boreskov Institute of Catalysis, Siberian Division, Russian Academy of Sciences, Novosibirsk, 630090 Russia

Received March 26, 2001

Abstract—The effect of the conditions of thermal treatment on the texture formation in molybdenum–titanium oxide (Mo–Ti–O) and vanadium–molybdenum–titanium oxide (V–Mo–Ti–O) catalysts was studied. It was found that the presence of MoO_3 in the Mo–Ti–O catalyst resulted in the stabilization of the surface area of anatase and in the retention of the fine pore structure upon thermal treatment because of the insertion of highly dispersed molybdenum crystallites into the aggregates of anatase crystallites, preventing from their agglomeration over a wide range of temperatures. In the presence of MoO_3 and V_2O_5 in the catalyst, anatase particles underwent agglomeration as the temperature was increased. This resulted in a more drastic decrease in the specific surface area and an increase in the pore size, as compared with binary samples, because of the formation of a thermally labile vanadium–molybdenum compound at the surface of anatase.

INTRODUCTION

Vanadium–titanium oxide catalysts modified with molybdenum and molybdenum–titanium oxide catalysts are used in a number of important processes of partial oxidation. For example, molybdenum–titanium catalysts exhibit high activity in the partial oxidation reactions of toluene [1], olefins [2], and alcohols [3]. Vanadium–titanium catalysts with molybdenum additives are active and selective in a number of partial oxidation reactions, such as benzene oxidation to maleic anhydride [4–6], *ortho*-xylene oxidation to phthalic anhydride [7, 8], and toluene oxidation to benzaldehyde [9]. It is also well known [10–12] that these catalysts also exhibit high activity in the selective reduction of nitrogen oxides with ammonia.

We should focus our attention on an improvement in the stability of a vanadium–titanium catalyst in a reaction mixture upon catalyst modification with molybdenum [12]. Although few data on the formation of an active component of these catalysts were published [13, 14], the formation of their pore structures was almost not studied.

The aim of this work was to examine the effect of the conditions of thermal treatment of Mo–Ti–O and V–Mo–Ti–O catalysts on the formation of pore structures over a wide range of temperatures.

EXPERIMENTAL

A Mo–Ti–O catalyst with the composition 10 wt % MoO_3 and 90 wt % TiO_2 was synthesized by the mixing of titanium hydroxide (anatase), which was prepared by the industrial sulfuric acid technology [15], and an ammonium paramolybdate solution followed by spray drying, the pelletization of the resulting powder, and thermal treatment at 110–700°C in a flow of air.

The V–Mo–Ti–O catalyst with the composition 20 wt % V_2O_5, 5 wt % MoO_3, and 75 wt % TiO_2 was synthesized by the mixing of titanium hydroxide (anatase) with ammonium paramolybdate and vanadyl oxalate solutions followed by spray drying, pelletization, and thermal treatment at 200–700°C in a flow of air. In the course of high-temperature calcination for 4 h, the catalysts exhibited no detectable changes in the chemical composition because of the volatility of their components. The concentrations of V and Mo were determined by atomic absorption spectrometry on a Saturn spectrometer.

The pore structure of the prepared catalysts was studied by the low-temperature (77.4 K) adsorption of nitrogen on a DigiSorb-2600 Micrometrics instrument. The true density ρ (g/cm^3) was measured on an AutoPycnometer-1320 Micrometrics instrument using helium. The total pore volume V_Σ (cm^3/g) and the porosity ε (cm^3/cm^3) were calculated from the bulk density δ (g/cm^3) and the true density by the commonly used relationships $V_\Sigma = (0.6/\delta - 1/\rho)$ and $\varepsilon = V_\Sigma\rho/(1 + V_\Sigma\rho)$. The limiting sorption-space volume V_s (cm^3/g), that is, the micro- and mesoporous part of the pore space, was directly determined from adsorption experiments. The meso- and macropore surface area S_α (m^2/g) and the micropore volume V_μ (cm^3/g) were determined by a comparative method of treating N_2 adsorption isotherms in accordance with a published

0023-1584/02/4304-0573$27.00 © 2002 MAIK “Nauka /Interperiodica”

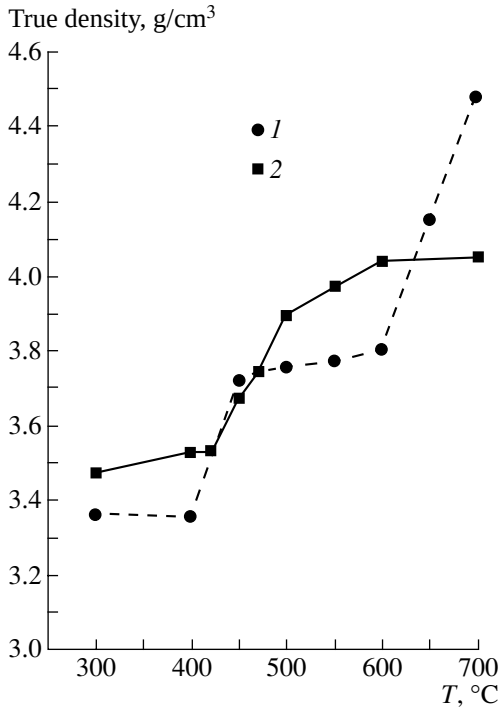

Fig. 1. True densities of (*1*) Mo–Ti–O and (*2*) V–Mo–Ti–O catalysts as functions of treatment temperature.

procedure [16]. The total surface area S (m^2/g) was measured by a rapid single-point method [16] from the thermal desorption of Ar. The average catalyst particle size was estimated by the relation $d = 6/S\rho$. The pore size distribution according to the equivalent sizes of pore entrances was calculated from the desorption branches of nitrogen adsorption isotherms by the Barrett–Joyner–Halenda method [17].

The X-ray diffraction analysis of the samples was performed on a URD-63 diffractometer with monochromatic CuK_α radiation. The size of coherent-scattering regions (CSR) was determined by the Scherrer formula using halfwidths of 1.0.1. and 2.0.0. diffraction peaks [18].

The electron-microscopic studies were performed on a JEM 2010 instrument with a resolution of 1.4 Å and an accelerating voltage of 200 kV.

RESULTS AND DISCUSSION

Molybdenum–Titanium Oxide Catalysts

Table 1 and Fig. 1 summarize data on the true density ρ and the pore structure parameters of a binary Mo–Ti–O catalyst depending on calcination temperature. It can be seen that the temperature dependence of ρ is represented by a complicated step curve: the true density was almost constant at 300–400°C; next, it increased in a temperature range of 400–450°C and remained constant at 450–600°C; as the temperature was increased above 600°C, the true density also sharply increased. This shape of the temperature dependence of ρ is indicative of a complex character of changes in the chemical and phase composition of the molybdenum–titanium catalyst in the course of thermal treatment.

We compared data on changes in the true density ρ with X-ray diffraction data and published data [19, 20] on changes in the true density and phase composition of pure titanium dioxide. This allowed us to conclude that, along with the anatase phase, an amorphous phase, whose true density is lower than the density of crystalline anatase, was present in the catalyst at a temperature lower than 400°C. This was due to the formation of an amount of low-molecular forms (polyhydroxo complexes of the general formula $TiO_x(OH)_y^{[4-(2x-y)]^+}$ [15]) in addition to crystalline anatase particles in the synthesis of titanium dioxide by the sulfuric acid technology because of the incomplete hydrolysis of parent salts. These compounds are unstable, and they were retained only under comparatively mild conditions of thermal treatment. The further polycondensation of the polyhydroxo complexes took place with the formation of the anatase phase of titanium dioxide as the temperature was increased; because of this, ρ increased in the temperature range 400–450°C [20].

Table 1. Texture parameters of the Mo–Ti–O catalyst

T, °C	ρ, g/cm^3	δ, g/cm^3	V_Σ, cm^3/g	ε, cm^3/cm^3	S_α, m^2/g	V_μ, cm^3/g	V_s, cm^3/g	d, nm	ΔV, cm^3/g
300	3.36	0.70	0.55	0.65	138.1	0.024	0.255	12.9	–
400	3.35	0.67	0.60	0.67	163.8	0.012	0.279	10.9	–
450	3.72	0.66	0.64	0.70	189.6	0	0.302	8.5	0.03
500	3.75	0.66	0.64	0.71	173.8	0	0.270	9.1	–
550	3.77	0.68	0.61	0.70	137.0	0	0.292	11.6	–
600	3.80	0.72	0.56	0.68	89.7	0	0.278	17.6	–
650	4.15	0.73	0.57	0.70	65.0	0	0.274	22.2	0.02
700	4.48	0.70	0.63	0.74	11.2	0	0.099	119.6	0.02

According to X-ray diffraction data, the Mo–Ti–O sample calcined at 300–650°C contained only the phase of crystalline anatase. However, rutile and MoO_3 phases were also reliably detected upon the thermal treatment above 650°C. Consequently, it is believed that the increase in the true density at temperatures higher than 600°C was due to the formation and increase in the fraction of rutile and MoO_3 phases in the catalyst.

It was found previously [20] that the presence of products of the incomplete hydrolysis of parent titanium salts in titanium dioxide is also responsible for the occurrence of micropores. It follows from Table 1 that a noticeable micropore volume was detected in the molybdenum–titanium catalyst; this volume was retained on heating the catalyst up to 400°C and then disappeared, whereas micropores were not detected in pure titanium dioxide even at a temperature higher than 300°C. Consequently, the doping of titanium dioxide with molybdenum enhances the thermal stability of the binary oxide system and so increases the limiting temperature of the existence of the products of incomplete hydrolysis, which are responsible for the occurrence of micropores.

Figure 2 illustrates changes in the total specific surface area *S* of the test samples, as measured by the thermal desorption of argon. The specific surface area of titanium dioxide gradually decreased with temperature, whereas the surface area of the Mo–Ti–O sample remained almost unchanged up to 500°C; then, it dramatically decreased at higher temperatures.

It follows from the electron-microscopic data (Fig. 3) that the molybdenum–titanium sample calcined at 450–650°C consisted of highly dispersed anatase crystallites with a regular structure of size 3–8 nm;

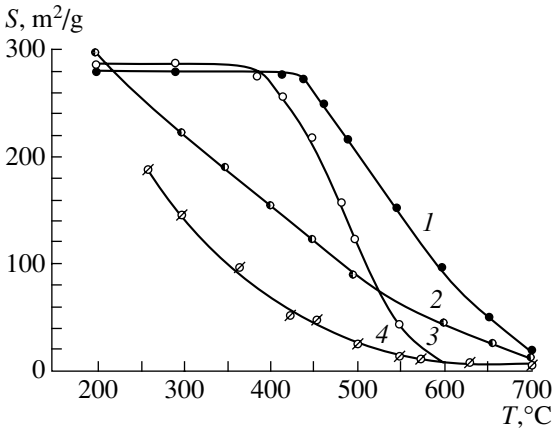

Fig. 2. Specific surface area (*S*) as a function of calcination temperature. Catalysts: (*1*) Mo–Ti–O, (*2*) pure titanium dioxide, (*3*) V–Ti–O, and (*4*) V–Mo–Ti–O.

these crystallites were incoherently grouped into coarser aggregates of size about 70–90 nm. Highly dispersed molybdenum oxide crystallites of size about 1–2 nm were observed between the anatase particles (Table 2). Strips observed in the micrographs are the images of a crystal lattice, and the distance between them corresponds to the interplanar spacing in a certain crystallographic direction. In this case, the micrograph exhibits the parameters $\lambda = 0.385$ nm, typical of the anatase lattice, and $\lambda = 0.304$ nm, typical of the MoO_3 structure in the (101) direction. The structural arrangement of this sample was changed after calcination at 700°C. Coarse (about 100 nm in size) rutile crystals and MoO_3 oxide particles of approximately the same size were observed.

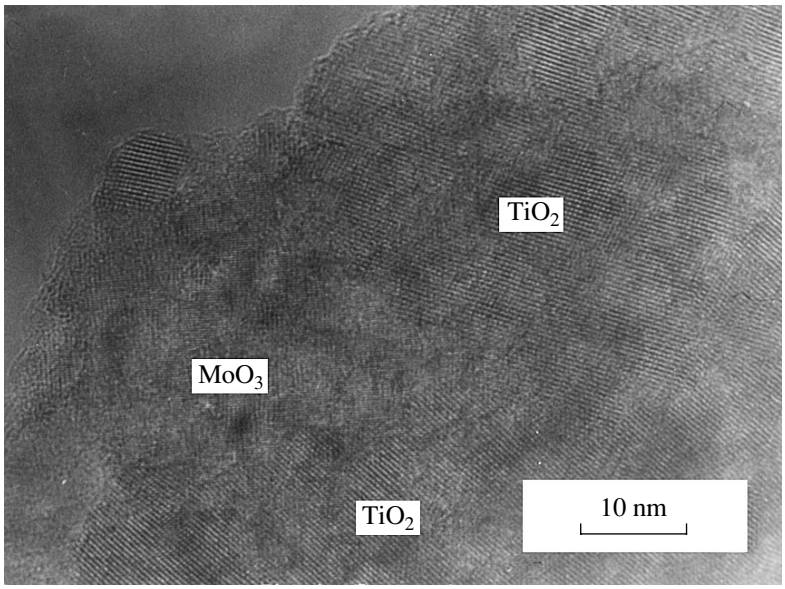

Fig. 3. Electron micrograph of the Mo–Ti–O catalyst calcined at 450°C.

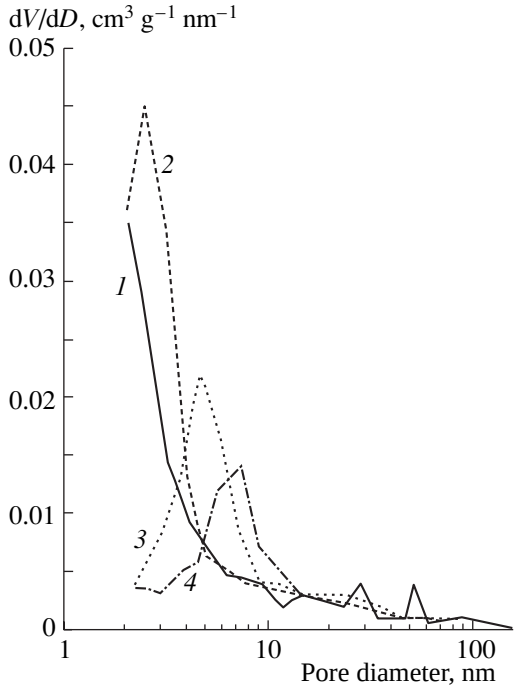

Fig. 4. Differential curves of pore-volume distribution according to the size of pore entrances for the Mo–Ti–O catalyst at different calcination temperatures: (*1*) 300, (*2*) 500, (*3*) 600, and (*4*) 650°C.

It follows from the X-ray diffraction data (Table 2) that the CSR size of anatase crystallites in the molybdenum–titanium sample calcined at 300–500°C was changed only slightly, and it was equal to 7.0–8.5 nm. A further increase in the temperature resulted in an increase in the CSR of anatase; this increase was most significant at 700°C. Table 1 also indicates that the averaged catalyst particle size *d*, which was obtained from adsorption data, is consistent with the CSR size; in this case, this comparison is essentially correct because the molybdenum content of the catalyst is low.

Table 2. Phase composition and the CSR sizes of the Mo–Ti–O and V–Mo–Ti–O catalysts depending on calcination temperature

Chemical composition, wt %	*T*, °C	Phase composition	CSR size, nm
10% MoO_3 : 90% TiO_2	300	anatase	7.0
	450	anatase + MoO_3	8.5
	500	anatase + MoO_3	8.5
	550	anatase + MoO_3	11.0
	600	anatase + MoO_3	16.5
	650	anatase + MoO_3	19.0
	700	rutile + MoO_3^*	45.0
5% MoO_3 : 20% V_2O_5 : 75% TiO_2	400	anatase + Φ_s	11.0
	450	anatase + Φ_s	16.0
	500	anatase + V_2O_5	26.0

Note: Φ_s is the surface phase of a vanadium–molybdenum compound.
* The MoO_3 phase detected by X-ray diffraction analysis.

Thus, the above data suggest that highly dispersed anatase crystallites are stabilized by molybdenum oxide particles, which prevent them from agglomeration, in the Mo–Ti–O catalyst over a wide temperature range of 300–500°C. Because of this stabilization, this catalyst retained a high specific surface area at sufficiently high temperatures, whereas anatase particles were intensely agglomerated in pure titanium dioxide as the temperature was increased. This resulted in a noticeable decrease in the oxide surface area even at a temperature of 250°C.

As follows from data given in Table 1, the thermal treatment of the Mo–Ti–O sample over the entire range of temperatures did not considerably affect the limiting sorption-space volume (V_s) up to 700°C; next, this value dramatically decreased. The porosity ε also remained almost constant over a temperature range of 400–650°C; however, it somewhat increased as the calcination temperature was increased above 650°C.

It is well known that the high-temperature agglomeration of xerogels primarily occurs by two mechanisms: surface diffusion and bulk flow [21]. As a rule, the former mechanism is predominant in the temperature range $(0.3–0.6)T_m$, whereas the latter is predominant at $T > 0.6T_m$, where T_m is the melting temperature of the xerogel material. The mechanism of surface diffusion results in a decrease in the surface area without a significant increase in the packing density of particles, that is, without a decrease in the porosity. Thus, the data suggest that in the thermal treatment of the catalyst at a temperature lower than 700°C agglomeration occurred by the surface diffusion mechanism, whereas catalyst agglomeration by the bulk flow mechanism was predominant at 700°C or above.

We compared data on changes in the true density, that is, a parameter that characterizes the phase composition of the test catalyst, and the porosity of samples. It can be seen that an increase in the porosity at a temperature higher than 650°C was due to a phase transition which occurred simultaneously with agglomeration. This phase transition was accompanied by an increase in the true density of the catalyst framework and, as a result, by the appearance of the additional pore volume $\Delta V \approx \Delta(1/\rho)$ (Table 1).

Figure 4 depicts the curves of differential pore-volume distribution according to the size of critical pore entrances for the binary molybdenum–titanium catalyst. It can be seen that the calcination of the sample at a temperature lower than 500°C did not result in a considerable change in the pore structure; only a further increase in the temperature was accompanied by a symbatic increase in the predominant pore size.

Note that an analogous dependence of the specific surface area and texture changes on calcination temperature was observed previously in vanadium–titanium catalysts [19]. For comparison, Fig. 2 demonstrates the specific surface areas of vanadium–titanium and molybdenum–titanium catalysts (at equal molar concentrations of V_2O_5 and MoO_3 oxides) as functions of calcination temperature. It can be seen that the thermal stability of titanium dioxide modified with molybdenum is higher than the thermal stability of titanium dioxide modified with vanadium. According to the ideas of Tamman (see, for example, [21]), it would be expected that Mo–Ti–O catalysts are more thermally stable than V–Ti–O catalysts. Indeed, the melting temperature of MoO_3 (795°C) is higher than that of V_2O_5 (675°C) [22]. Because of this, the particles of highly dispersed MoO_3 (which stabilizes the existence of highly dispersed anatase particles in aggregates) undergo agglomeration at a higher temperature, as compared with highly dispersed vanadium oxide particles (which stabilize anatase particles in vanadium–titanium catalysts); this was supported experimentally. In pure titanium dioxide in the absence of a highly dispersed phase of molybdenum oxide (which prevents the agglomeration of anatase particles), anatase particles are rapidly agglomerated as the temperature increases. Anatase crystallites can also be doped with molybdenum ions because of the imperfection of the crystal lattice of parent titanium dioxide. According to Reznitskii [23], this can also enhance their thermal stability because of an increase in the energy of local metal–oxygen bonds in the surface layer of catalyst particles.

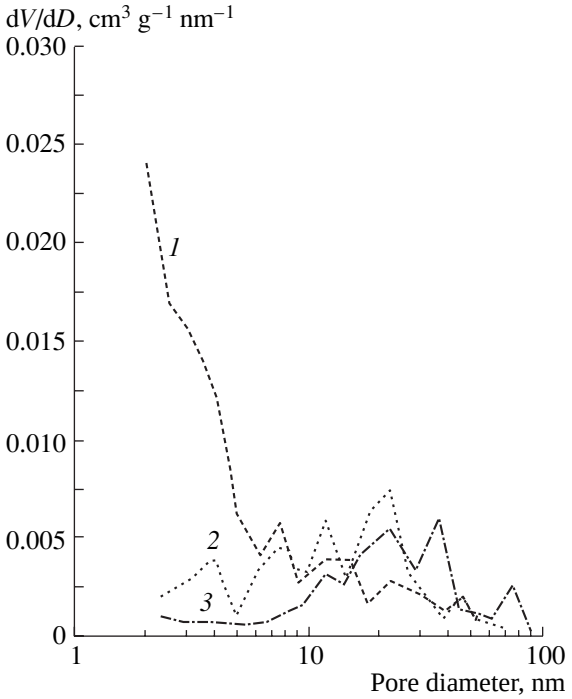

Fig. 5. Differential curves of pore-volume distribution according to the size of pore entrances for the V–Mo–Ti–O catalyst at different calcination temperatures: (*1*) 400, (*2*) 450, and (*3*) 500°C.

Vanadium–Molybdenum–Titanium Oxide Catalysts

Table 3 and Fig. 2 summarize the texture parameters of the V–Mo–Ti–O catalyst and the temperature dependence of its specific surface area. It can be seen that this dependence for the ternary catalyst is different from that for binary vanadium–titanium and molybdenum–titanium catalysts. Figure 2 indicates that the specific surface area of the V–Mo–Ti–O sample significantly decreased with temperature; this decrease was even more drastic than that in pure titanium dioxide.

According to X-ray diffraction and electron-microscopic data, only an anatase phase was detected in the samples calcined at temperatures lower than 400°C, whereas weakly intense lines of the surface vanadium–molybdenum compound Φ_s were detected along with anatase in the temperature range 400–470°C (Table 2). The structure of this compound was described elsewhere [24]. As the temperature was further increased up to 500°C, the formation of a V_2O_5 phase was detected along with the anatase phase. A constant

Table 3. Texture parameters of the V–Mo–Ti–O catalyst

T, °C	ρ, g/cm^3	δ, g/cm^3	V_Σ, cm^3/g	ε, cm^3/cm^3	S_α, m^2/g	V_s, cm^3/g	*d*, nm
110	2.76	0.80	0.388	0.517	–	–	–
300	3.47	0.84	0.426	0.597	–	–	12.1
400	3.53	0.80	0.467	0.622	97.7	0.197	29.8
420	3.53	0.82	0.448	0.612	–	–	32.1
450	3.67	0.73	0.548	0.668	39.2	0.229	35.5
470	3.74	0.73	0.553	0.674	39.9	0.212	51.7
500	3.89	0.74	0.558	0.682	27.5	0.241	68.0
550	3.93	0.73	0.568	0.690	–	–	76.2
600	4.10	0.78	0.526	0.680	–	–	185.2
700	4.10	1.64	0.123	0.335	–	–	665.1

increase in the true density ρ with calcination temperature at $T > 400$°C (Fig. 1) is also indicative of a comparatively narrow temperature range of the existence of the detected intermediate phases and a gradual change in the phase composition of the sample.

The measurement of the CSR sizes of anatase demonstrated that they increased with calcination temperature (Table 2) because of the gradual agglomeration of anatase particles over the entire range of temperatures.

The catalyst particle size (d), which was calculated from adsorption data, continuously increased in the course of calcination. This increase was most significant at a temperature of 600°C or higher. A comparison of the particle size obtained from adsorption data and the CSR size is indicative of the block structure of catalyst particles; this is also consistent with previous data [24]. It follows from the above data and the electron micrograph of the V–Mo–Ti–O test sample (which was published in [24]) that anatase particles are incoherently agglomerated over a temperature range of 350–470°C, whereas in the case of pure titanium dioxide anatase particles are coherently agglomerated over a wide range of treatment temperatures (300–800°C) [25]. It is likely that the change in the agglomeration mechanism of anatase particles in the V–Mo–Ti–O sample is indicative of the modification of anatase particles with molybdenum and vanadium with the formation of the surface compound Φ_s at the first stage and with the subsequent formation of a bulk compound. This modification may be responsible for the lower thermal stability of anatase in the course of thermal treatment. The above data indicate that this results in a more drastic decrease in the specific surface area with temperature. The absence of a detectable micropore volume even at temperatures higher than 300°C is also indicative of the higher mobility of the surface layers of the catalyst. The nature of the modification of titanium dioxide with vanadium and molybdenum requires a more detailed study, which will be performed in the future.

Data on changes in the pore volume V_Σ and the porosity ε (Table 3) indicate that the agglomeration of the V–Mo–Ti–O sample at temperatures lower than 700°C primarily occurred by the surface diffusion mechanism, whereas the agglomeration of catalyst particles occurred by the bulk flow mechanism with a considerable decrease in the porosity of the catalyst at a temperature of 700°C or higher.

Figure 5 depicts the curves of pore-volume distribution according to the size of pore entrances for the V–Mo–Ti–O catalyst calcined at different temperatures. It can be seen that, in this case, an increase in the calcination temperature resulted in a symbatic increase in the predominant pore size.

Thus, the results of this study suggest that the textures of Mo–Ti–O and V–Mo–Ti–O catalysts are formed in significantly different manners. At the same time, the above results and previously published data [19] on the formation of the V–Ti–O system allowed us to conclude that the formation of the dispersity and texture of the binary vanadium–titanium and molybdenum–titanium systems on thermal treatment is described by the same physicochemical laws.

In both binary systems, the formation of highly dispersed vanadium or molybdenum oxide crystallites, which are uniformly distributed in the bulk of the catalyst between highly dispersed anatase crystallites, on thermal treatment prevents anatase agglomeration and improves the thermal stability of the catalyst by stabilizing its developed surface at sufficiently high temperatures. In the absence of the stabilizing additives of molybdenum or vanadium, the particle size of anatase gradually increases because of agglomeration as the temperature of calcination is increased.

The data also indicate that the chemical nature of the additive significantly affects the thermal stability of the system as a whole: anatase particles in the Mo–Ti–O system undergo agglomeration at a higher temperature than in the V–Ti–O system. In other words, the higher the melting temperature of a stabilizing additive, the higher the temperature at which its stabilizing effect is retained (which disappears only as a result of the agglomeration of the additive). In this context, it would be expected that, for example, the tungsten–titanium system will exhibit a higher thermal stability than the thermal stability of the Mo–Ti–O and V–Ti–O systems.

In the case of the ternary V–Mo–Ti–O catalyst, because of the absence of the bulk highly dispersed additive of an oxide phase from the system, as a consequence of the formation of a thermally labile surface vanadium–molybdenum compound, anatase crystallites undergo rapid agglomeration as the temperature of calcination is increased. This results in a dramatic decrease in the surface area and a texture transformation.

REFERENCES

1. Nag, N.K., Fransen, T., and Mars, P., *J. Catal.*, 1981, vol. 68, no. 1, p. 77.
2. Mamoru, Ai., *J. Catal.*, 1978, vol. 54, no. 3, p. 426.
3. Vanhove, D., Op, S.R., Fernandes, A., and Blaachard, M., *J. Catal.*, 1979, vol. 57, no. 2, p. 253.
4. Satsuma, A., Okada, F., Yattori, A., Miyamoto, A., Hattori, T., and Mirakami, Y., *Appl. Catal.*, 1991, vol. 72, no. 2, p. 295.
5. Najbar, M., *J. Chem. Soc., Faraday Trans. 1*, 1986, vol. 82, no. 10, p. 1673.
6. Lui, Z.X., Li, Y.Q., Qi, S.X., Xie, K., Wu, N.J., and Bao, Q.X., *Appl. Catal.*, 1989, vol. 56, no. 2, p. 207.
7. Nikolov, V., Klissurski, D., and Anastasov, A., *Catal. Rev.–Sci. Eng.*, 1991, vol. 33, nos. 3–4, p. 319.
8. US Patent 14481304, 1984.
9. Matralis, H.K., Papadoponlou, Ch., Kordulies, Ch., Elguezabel, A.A., and Corberan, V.C., *Appl. Catal. A*, 1995, vol. 126, no. 2, p. 365.

10. Orlik, S.N., Ostanyuk, V.A., and Martsenyuk-Kukharuk, M.G., *Kinet. Katal.*, 1995, vol. 36, no. 2, p. 311.
11. Hilbrid, F., Gobel, H.E., Knozenger, H., Schmelz, H., and Lengeler, B., *J. Catal.*, 1991, vol. 129, no. 1, p. 168.
12. Busca, G., Lietti, L., Ramis, G., and Derti, F., *Appl. Catal. B*, 1998, vol. 18, nos. 1–2, p. 1.
13. Busca, G. and Marchetti, L., *J. Chem. Res. Synop.*, 1986, no. 5, p. 174.
14. Lange, F.C., Schmelz, H., and Knozenger, H., *Appl. Catal. B*, 1996, vol. 8, no. 1, p. 245.
15. Dobrovol'skii, I.P., *Khimiya i tekhnologiya oksidnykh soedinenii titana* (Chemistry and Technology of Oxide Compounds of Titane), Sverdlovsk: Izd-vo UrO AN SSSR, 1988.
16. Karnaukhov, A.P., *Adsorbtsiya. Tekstura dispersnykh i poristykh materialov* (Adsorption: Texture of Dispersed and Porous Materials), Novosibirsk: Nauka, 1999.
17. Gregg, S.J. and Sing, K.S.W., *Adsorption, Surface Areas, and Porosity*, New York: Academic, 1982.
18. Guinier, A., *Theorie et Technique de la Radiocristallographie*, Paris: Dunot, 1956.
19. Zenkovets, G.A., Gavrilov, V.Yu., Kryukova, G.N., and Tsybulya, S.V., *Kinet. Katal.*, 1998, vol. 39, no. 1, p. 122.
20. Gavrilov, V.Yu. and Zenkovets, G.A., *Kinet. Katal.*, 1993, vol. 34, no. 2, p. 357.
21. German, R.M. and Muniz, Z.A., *Sintering and Catalysis*, New York, 1975, p. 259.
22. Perel'man, V.I., *Kratkii spravochnik khimika* (Abridged Handbook of Chemistry), Moscow: Khimiya, 1964, pp. 80, 96.
23. Reznitskii, L.A., *Zh. Fiz. Khim.*, 2000, vol. 74, no. 5, p. 823.
24. Kryukova, G.N., Zenkovets, G.A., and Parmon, V.N., *React. Kinet. Catal. Lett.*, 2000, vol. 71, no. 1, p. 173.
25. Zenkovets, G.A., Tsybulya, S.V., Burgina, E.B., and Kryukova, G.N., *Kinet. Katal.*, 1999, vol. 40, no. 4, p. 623.